Acta Cryst. (1970). A**26**, 71

Anisotropic Extinction Corrections in the Zachariasen Approximation*

BY PHILIP COPPENS† AND WALTER C. HAMILTON

Chemistry Department, Brookhaven National Laboratory, Upton, New York 11973, *U.S.A.*

(*Received* 7 *February* 1969)

Refinement of crystal structures incorporating an extinction parameter in an approximation developed by Zachariasen has led to the experimental observation that some crystals show anisotropic extinction effects. A formalism is presented for refinement of anisotropic extinction coefficients for both extreme crystal types: Type I (extinction dominated by mosaic spread) and Type II (extinction dominated by particle size). For Type I crystals, an anisotropic rather than isotropic Gaussian mosaic spread distribution function is assumed. For Type II crystals, the average particle shape is described as an ellipsoid rather than as a sphere. In each case, the six independent components of a symmetrical second-order tensor are added to the list of parameters refined in a conventional crystallographic least-squares program. Results on several data sets from both neutron and X-ray diffraction experiments indicate that anisotropy of extinction is often significant. The inclusion of such parameters is recommended in all least-squares refinements of extinction affected data. Furthermore the detailed study of the effects may be of some promise in the study of crystal texture inasmuch as the refined parameters are of a magnitude which suggests physical significance.

Introduction

Zachariasen (1967) has given a general treatment of secondary extinction and introduced some useful approximations which allow the facile introduction of the extinction correction into calculation of Bragg intensities in crystal structure refinements. The use of the Zachariasen approximation has proved to be satisfactory in the analysis of a number of crystal structures (Zachariasen, 1968*a*) while Larson (1967), and Ibers (1968) successfully applied an earlier expression of Zachariasen (1963) in least-squares refinements of intensity data. For reference later in the paper, it is useful to summarize the Zachariasen treatment here.

The integrated intensity of a diffracted beam is given by

$$\mathscr{P}=\mathscr{P}_k y‡ \qquad (1)\ (Z\text{-}1)$$

with

$$\mathscr{P}_k=\mathscr{I}_0 v A(\mu) Q \qquad (2)\ (Z\text{-}2a)$$

$$Q(\text{X-ray})=\left|\frac{e^2FK}{mc^2V}\right|^2 \frac{\lambda^3}{\sin 2\theta} \qquad (3)\ (Z\text{-}2b)$$

and

$$Q(\text{neutron})=\left|\frac{FK}{V}\right|^2 \frac{\lambda^3}{\sin 2\theta}\,. \qquad (4)$$

Formulas (3) and (4) are valid if the structure factor F is expressed in electrons cell^{-1} for X-rays and cm cell^{-1} for neutrons. The polarization factor K is equal to 1 for neutrons but is either 1 or cos 2θ for the normal and parallel components of polarization for X-rays. The power equations (with appropriate boundary conditions) in the absence of absorption:

$$\frac{\partial I_0}{\partial t_1}=-\sigma I_0+\sigma I \qquad (5)\ (Z\text{-}4a)$$

$$\frac{\partial I}{\partial t_2}=-\sigma I+\sigma I_0\ , \qquad (6)\ (Z\text{-}4b)$$

have a solution that depends on the crystal shape. (See, for example, Hamilton, 1957, 1963.) Zachariasen avoids the difficulty of solution of these equations in the general case by making three approximations:

(1) The power diffracted in a direction ε from a single domain for any crystal shape is given by

$$P(\varepsilon)=\mathscr{I}_0 v\sigma(\varepsilon)\varphi\{\sigma(\varepsilon)\} \qquad (7)\ (Z\text{-}7,8)$$

and

$$\varphi\{\sigma(\varepsilon)\}=\frac{1}{(1+\sigma(\varepsilon)\bar{t})} \qquad (8)\ (Z\text{-}19)$$

where $\bar{t}$ is the mean path length in a single domain for the reflection in question. A similar approximation is made for the whole crystal.

(2) The Laue form of the peak profile function may be replaced by a Poisson function.

(3) The effects of absorption are accounted for by using in the extinction equations an effective mean path length, $\bar{T}$, through the crystal that is obtained as follows

$$\bar{T}=\frac{1}{A(\mu)}\int (T_1+T_2)\exp\left[-\mu(T_1+T_2)\right]d\tau \qquad (9)$$

where $d\tau$ implies integration over all diffraction paths in the crystal with all volume elements being given equal weight.

* Research carried out at Brookhaven National Laboratory under contract with the U.S. Atomic Energy Commission.

† Present address: Chemistry Department, State University of New York at Buffalo, Buffalo, New York 14214, U.S.A.

‡ All symbols used in this paper are summarized in the Appendix.

Zachariasen's final results may be summarized as

$$\mathscr{P}=\mathscr{P}_k y=\mathscr{I}_0 Q_0 p_1 v A(\mu) y \quad (10)\ (\text{Z-46}a)$$

$$y=\{1+(2p_2/p_1)\bar{x}_0\}^{-1/2} \quad (11)\ (\text{Z-45})$$

$$\bar{x}_0=\beta Q_0[\bar{t}+(\bar{T}-\bar{t})\{1+(\beta/g)^2\}^{-1/2}] \quad (12)\ (\text{Z-46}c)$$

$$\beta=2\bar{t}_\perp/3\lambda\,. \quad (13)\ (\text{Z-46}d)$$

The quantity g is related to the width of the mosaic spread distribution. If primary extinction may be neglected (as is often the case):

$$\bar{x}_0=\beta Q_0\bar{T}\{1+(\beta/g)^2\}^{-1/2}\,. \quad (14)\ (\text{Z-48})$$

For a spherical domain of radius r,

$$\bar{t}_\perp=\bar{t}=\pi r/2\,, \quad (15)$$

and hence

$$\beta=\frac{\pi}{3}(r/\lambda)\simeq r/\lambda\,. \quad (16)$$

If $\beta\gg g$

$$\bar{x}_0=gQ_0\bar{T} \quad (17)\ (\text{Z-49}a)$$

and the extinction is dependent only on the mosaic spread parameter η and not on the mosaic block size. For such a crystal, defined by Zachariasen as Type I, the mosaic spread parameter η is considerably larger than the natural width of the reflection from a single domain.

If $\beta\ll g$,

$$\bar{x}_0=\beta Q_0\bar{T}\,. \quad (18)\ (\text{Z-49}b)$$

For such a crystal, defined by Zachariasen as Type II, the natural width of the reflection from a single domain is greater than the mosaic spread parameter. Since it is again the convolution of the two that matters, there is no dependence on the mosaic spread parameter. Real crystals may lie between the two extremes. Without measurements at different wavelengths, or except for the case of extreme anisotropy, it is impossible to distinguish between the two types on the basis of diffraction measurements alone.

We have found in applying the Zachariasen correction to several sets of data that there are pronounced anisotropic effects. For example, the $0k0$ reflections may be always undercorrected and the $h0l$ reflections may always be overcorrected. It seemed desirable to include this effect in the calculation of the intensities and to refine appropriate ansiotropic extinction parameters in the least-squares refinements.

Formulation of anisotropic extinction

The Zachariasen formulation includes two parameters which describe the mosaic character of the crystal: $\bar{t}$ is a measure of the domain size; g is a parameter in a Gaussian mosaic angle distribution. A reasonable extension to anisotropy is to assume that the domain is no longer spherical but ellipsoidal and that the mosaic spread is no longer isotropic but is given by an anisotropic Gaussian function. In the formulation that follows, these are the assumptions that are made.

The particle shape enters equations (Z-46) in two places, once in $\bar{t}$, the mean path length in the domain, and secondly in $\bar{t}_\perp$, the mean dimension in the domain in a direction lying in the plane of diffraction and perpendicular to the incident beam. In the present formulation, we choose to assume that primary extinction is negligible; hence the effect of any anisotropy of particle shape on t will be unimportant.

The particle shape may be described by the expression for an ellipsoid:

$$\mathbf{X}'\mathbf{W}\mathbf{X}=1\,, \quad (19)$$

where $\mathbf{X}$ are the coordinates relative to some axis system with metric $\mathbf{G}^*$ and $\mathbf{W}$ is a second order metric tensor. The half-dimension through the center of the particle in a direction specified by a unit vector N is

$$r(\mathbf{N})=(\mathbf{N}'\mathbf{W}\mathbf{N})^{-1/2}\,. \quad (20)$$

The mean length $\bar{t}_\perp$ for an ellipsoidal particle is given by

$$\bar{t}_\perp=\frac{\pi}{2}r(\mathbf{N})\,. \quad (21)$$

If we can determine the components of the tensor $\mathbf{W}$, we may reduce it to a principal axis system by finding its eigenvalues and eigenvectors in a space of metric $\mathbf{G}$. The appropriate equation for the eigenvalues is

$$|\mathbf{W}-\Lambda G|=0\,. \quad (22)$$

The inverse square roots of the eigenvalues then give the half-lengths of the principal axes of the average ellipsoidal domain.

The anisotropy of particle shape is thus introduced into equation (Z-48) by finding the vector $\mathbf{N}$ which lies in the plane of the incident and diffracted beams but which is perpendicular to the incident beam and calculating

$$\beta=\frac{2\bar{t}}{3\lambda}=\frac{2}{3}\frac{\pi r(\mathbf{N})}{2\lambda}\simeq\frac{r(\mathbf{N})}{\lambda}\,. \quad (23)$$

For each reflection, we thus replace $\mathbf{r}$ in Zachariasen's formulation by $r(\mathbf{N})$ as calculated from (20).†

---

* In our least-squares programs we normally use the metric

$$\begin{bmatrix} 1 & \cos\gamma & \cos\beta \\ \cos\gamma & 1 & \cos\alpha \\ \cos\beta & \cos\alpha & 1 \end{bmatrix}$$

where α, β and γ are the unit-cell angles.

† Implicit in this procedure is the assumption that the 'feedback' term I in [the expression (Z-4) is negligible. In the anisotropic case these expressions are no longer symmetric. (Z-4a) becomes: $\dfrac{\partial I_0}{\partial t_1}=\sigma(\varepsilon_1)I_0+\sigma(\varepsilon_2)I$ where ε_1 and ε_2 are the incidence and reflectance directions and $\sigma(\varepsilon_1)$ and $\sigma(\varepsilon_2)$ depend respectively on the particle sizes in the directions of $\mathbf{N}$, and in the direction of a second vector $\mathbf{n}$ perpendicular to the diffracted beam in the plane of the incident and diffracted beams. As a result, extinction will also depend on the particle size in the direction of $\mathbf{n}$. This dependence is small because $I_0\gg I$, for crystals used in structure analyses.

The anisotropy of mosaic spread may be handled in the following way. Zachariasen assumes a Gaussian probability distribution in the angular parameter Δ:

$$\psi(\Delta)=2^{1/2}g\exp(-2\pi g^2\Delta^2)\,. \tag{24}$$

We introduce an anisotropic Gaussian

$$\psi(\Delta,\mathbf{D})=|Z|^{1/2}2^{3/2}\exp(-2\pi\mathbf{D}'Z\mathbf{D}\Delta^2) \tag{25}$$

where **D** is a unit vector (in a space with metric **G**) which is perpendicular to the plane which contains the incident and diffracted beams. The mosaic spread parameter in this plane is given by

$$\eta(\mathbf{D})=\frac{1}{2\pi^{1/2}}(\mathbf{D}'Z\mathbf{D})^{-1/2}\,. \tag{26}$$

The tensor **Z** may be diagonalized as was the tensor **W** to obtain the principal components of the mosaic spread probability function. The appropriate equation is $|Z-\Lambda G|=0$. The inverse square roots of the eigenvalues divided by $2\pi^{1/2}$ are the principal components of the mosaic spread probability function η_1,η_2,η_3.

We introduce the anisotropic mosaic spread parameters into equation (Z-48) by finding the vector **D** which is perpendicular to the plane of the incident and diffracted beams and calculating $g(\mathbf{D})=(\mathbf{D}'Z\mathbf{D})^{1/2}$. We could thus write (Z-48) as

$$\bar{x}_0=r(\mathbf{N})\lambda^{-1}Q_0\bar{T}\left[1+\left\{\frac{r(\mathbf{N})}{\lambda g(\mathbf{D})}\right\}^2\right]^{-1/2}\,. \tag{27}$$

Since each reflection will have a characteristic pair of vectors **N** and **D** associated with it, it becomes possible to refine simultaneously the components of **W** and **Z**. (This is not possible in the isotropic case for data taken at a single wavelength because of the degeneracy of r and g.) Our experience suggests to us however that this simultaneous refinement would not be a fruitful approach except in extremely anisotropic cases. We accordingly confine our discussion below to anisotropic Type I crystals:

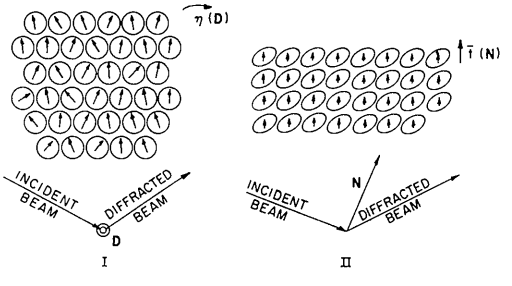

Fig. 1. Idealized models for anisotropic extinction. For Type I anisotropy the mosaic spread parameter η is not the same around all directions **D**. The shapes of the individual mosaic blocks are irrelevant. For Type II anisotropy, the particles are ellipsoidal. The mean radius varies with the direction **N**. In real crystals, both effects may be present. Classification as types I, II or intermediate depends on the relative values of the parameters η and $\bar{r}$.

$$r(\mathbf{N})/\lambda g(\mathbf{D})\gg 1 \tag{28}$$

$$\bar{x}_0=g(\mathbf{D})Q_0\bar{T} \tag{29}$$

and anisotropic Type II crystals:

$$r(\mathbf{N})/\lambda g(\mathbf{D})\ll 1 \tag{30}$$

$$\bar{x}_0=r(\mathbf{N})\lambda^{-1}Q_0\bar{T}\,, \tag{31}$$

with the realization (Zachariasen, 1969) that many crystals are likely to be intermediate in character. In Fig. 1, we illustrate schematically the two extreme types of anisotropic extinction.

Introduction of anisotropic into least-squares refinements

We have introduced both isotropic and anisotropic extinction refinement into our standard least-squares program (program *LINUS*, available on request). This is easy to do, but since the derivations of the derivatives are somewhat tedious and subject to error, we reproduce in Table 1 the necessary formulas.

Scaling

Because of the magnitudes of the quantities involved, we have found it convenient to scale γ, g, W_{ij}, and Z_{ij} as follows. We work throughout with the quantities:

$$\begin{aligned}\gamma'&=\gamma\times 10^4\,,\\ g'&=g\times 10^{-4}\,,\\ Z'_{ij}&=Z_{ij}\times 10^{-8}\,,\\ W'_{ij}&=W_{ij}\times\lambda^2\times 10^{-8}\ (\text{with }\lambda\text{ in Å}).\end{aligned} \tag{32}$$

Then all the previous equations hold without change on replacing the unprimed quantities by the primed quantities.

At the end of a refinement, we find that the following relations then hold:

Isotropic

Equivalent mosaic spread parameter

$$\eta=5{\cdot}8186/g'\ \text{seconds}\,.$$

Equivalent spherical domain radius

$$r=g'\lambda\cdot 10^{-4}\ (\text{with }\lambda\text{ in Å})\,. \tag{33}$$

*Type 1 anisotropic**

$$\Delta_i^{1/2}=\eta_{ii}(\text{seconds})=5{\cdot}8186/Z'^{1/2}_{ii}\,. \tag{34}$$

*Type 2 anisotropic**

$$\Delta_i^{1/2}=r_{ii}(\text{cm})=\lambda\,(\text{Å})\times 10^{-4}/W'^{1/2}_{ii}\,. \tag{35}$$

Convergence

We have found that refinement of an isotropic extinction parameter always proceeds smoothly to con-

* The principal axes of the ellipsoids may be interpreted in this way.

vergence, even starting from $g=0$. Anisotropic Type I refinements usually are well behaved starting from $Z_{ij}=0$. Anisotropic Type II refinements often go bad if starting from $W_{ij}=0$† or at any considerable distance from the correct value. We have always attained satisfactory results when we have first refined an isotropic parameter to convergence, then changed to anisotropic and continued.

Nevertheless, we have found that certain procedures facilitate convergence, particularly when starting from zero, which in some sense is an infinitely bad first approximation. Since the derivatives involve the value of $g(\mathbf{D})$ or $r(\mathbf{N})$, and since this may change markedly in one cycle of refinement, we have used the following partial-(or super full)-shift criterion:

If

$$|\delta W_{ii}| \text{ (or } |\delta Z_{ii}|) > \tfrac{1}{2} W_{ii}(\text{old})$$

then

$$W_{ii}(\text{new}) = W_{ii}(\text{old}) + \left[1 + \frac{\delta W_{ii}}{2W_{ii}(\text{old})}\right] \delta W_{ii}\,, \quad (36)$$

where δW_{ii} is the indicated shift obtained from the least-squares equations. Furthermore, if the calculated shift would make the diagonal term negative, we make the new W_{ii} or Z_{ii} equal to half the old one. When starting from far off the off-diagonal terms W_{ij} or Z_{ij} may behave badly, but since they may be either positive or negative, there is no condition such as that applied for the diagonal elements that completely prevents bad behavior. We have found useful an algorithm that does not allow a large shift if there is an indicated change in sign of W_{ij} (or Z_{ij}):

if

$$p_{\text{old}} \times (p_{\text{old}} + \delta p) < -0{\cdot}1 \quad (37)$$

we set instead

$$p_{\text{new}} = \tfrac{1}{2} p_{\text{old}}\,.$$

An additional feature of our least-squares programs is the print-out of the extinction correction for each reflection if it is less than or equal to 0·99. We also print out the equivalent mosaic spread for the diagonal elements of Type I crystals, the equivalent particle size for the diagonal elements for Type II crystals, and both for isotropic refinement.

Our data processing programs compute the necessary vectors **N** and **D** for each reflection. $\bar{T}$ is also calculated as

$$\bar{T} \simeq -\frac{\log A}{\mu} \quad (38)$$

which is equivalent to the approximation made by Zachariasen, an approximation that can be poor for crystals with high absorption. Furthermore, in crystals with high absorption ($\mu R > 0{\cdot}5$), and with large coherently scattering blocks, the Borrmann effect and the corresponding modified values of μ must be explicitly considered (Zachariasen, 1968*b*). If the extinction refinement is carried out to learn something about the mosaic character of crystals, it is thus best that crystals with low absorption be used.

† The derivative $\partial F^2/\partial W_{ij}$ is infinite for $\{W_{ij}\}=0$. When starting from $\{W_{ij}\}=0$ (which we rarely do) we usually replace $(\mathbf{N}'\mathbf{W}\mathbf{N})^{-3/2}$ by 1 for the first cycle.

Experimental results

Among a variety of compounds that we have studied recently by neutron and X-ray crystallography we have

Table 1. *Formula for extinction refinements*

(All symbols are defined in the *Appendix*)

γ is a quantity which depends on the mean path length, the polarization factors, the wavelength and the cell volume.

$$g = \begin{cases} g \text{ for isotropic extinction} \\ (\mathbf{D}'\mathbf{Z}\mathbf{D})^{1/2} \text{ for type 1 anisotropic extinction} \\ (\mathbf{N}'\mathbf{W}\mathbf{N})^{-1/2}/\lambda \text{ for type 2 anisotropic extinction} \end{cases}$$

$$y = \{1 - g\gamma F_c^2\}^{-1/2}$$

$$F_k = kF_c$$

$F^2 = k^2F_c^2y \equiv F_k^2y$	$F = kFy^{1/2} \equiv F_ky^{1/2}$
$\dfrac{\delta F^2}{\delta k} = y\dfrac{\delta F_k^2}{\delta k}$	$\dfrac{\delta F}{\delta k} = y^{1/2}\dfrac{\delta F_k}{\delta k}$
$\dfrac{\delta F^2}{\delta P} = \dfrac{y}{2}(y^2+1)\dfrac{\delta F_k^2}{\delta P}$	$\dfrac{\delta F}{\delta P} = \dfrac{y^{1/2}}{2}(y^2+1)\dfrac{\delta F_k}{\delta P}$
Isotropic	
$\dfrac{\delta F^2}{\delta g} = \dfrac{1}{2}k^2F_c^4y^3\gamma$	$\dfrac{\delta F}{\delta g} = \dfrac{1}{4}kF_c^3y^{5/2}\gamma$
Type 1 anisotropic	
$\dfrac{\delta F^2}{\delta Z_{ij}} = \dfrac{1}{4}k^2F_c^4y^3\gamma D_iD_j(\mathbf{D}'\mathbf{Z}\mathbf{D})^{-1/2}\{2-\delta_{ij}\}$	$\dfrac{\delta F}{\delta Z_{ij}} = \dfrac{1}{8}kF_c^3y^{5/2}\gamma D_iD_j(\mathbf{D}'\mathbf{Z}\mathbf{D})^{-1/2}\{2-\delta_{ij}\}$
Type 2 anisotropic	
$\dfrac{\delta F^2}{\delta W_{ij}} = -\dfrac{1}{4}k^2F_c^4y^3\gamma N_iN_j(\mathbf{N}'\mathbf{W}\mathbf{N})^{-3/2}\{2-\delta_{ij}\}\lambda$	$\dfrac{\delta F}{\delta W_{ij}} = -\dfrac{1}{8}kF_c^3y^{5/2}\gamma N_iN_j(\mathbf{N}'\mathbf{W}\mathbf{N})^{-3/2}\{2-\delta_{ij}\}\lambda$

found several for which anisotropic extinction effects are important. Some examples follow.

Since anisotropic extinction is not necessarily the same for symmetry related reflections, we have averaged only observations for reflections related by Friedel's law when data corresponding to more than one asymmetric unit in reciprocal space had been collected.

$B_{12}P_2$

This rhombohedral structure has been studied by La Placa (1968) who has collected a nearly complete hemisphere ($\frac{2}{3}$ of all reflections out to $\sin\theta/\lambda=0{\cdot}7$) of very accurate diffraction data from a spherical crystal with low absorption ($\mu=7{\cdot}313\ cm^{-1}$) on a General Electric-Datex automatic diffractometer. Isotropic, anisotropic Type I, and anisotropic Type II models were refined. The refinements converged (for 512 reflections, 131 of which were independent) with R values as indicated in Table 2 together with the final values of the refined extinction parameters. Using an R ratio test (Hamilton, 1965), the improvement on going to anisotropic extinction is significant. There is little difference in agreement between the Type I and Type II refinements, although the Type I refinement gives a slightly better result. To confirm the consistency of the results, the intensities of the 101 and 202 reflections were measured as a function of rotation around the scattering vector. With the extinction parameters determined from the full data set, intensities were calculated for the 101 and 202 reflections as a function of the rotational angle α. At low values of 2θ, the vector **N** which is relevant for Type II extinction lies nearly parallel to the scattering vector and thus varies little with rotation around this vector. Thus little variation in intensity (for a spherical crystal) is indicated if

Table 2. *Anisotropic extinction in X-ray data for* $B_{12}P_2$

Crystal data: rhombohedral $a=5{\cdot}248$ Å, $\cos\alpha=0{\cdot}3499$
Worst extinction: $F_{obs}^2/F_{calc}^2=0{\cdot}53$; $v=5\times10^{-4}$ mm³; $\lambda=0{\cdot}7107$ Å

Type I (unconstrained)

Z_{ij}'

11	22	33	12	13	23
6·4 (13)	1·7 (8)	4·3 (10)	1·8 (9)	1·0 (7)	1·0 (8)

Principal axes and directions

$\langle\eta_i\rangle$	Direction cosines*		
2·4″	−0·86	0·12	0·50
3·1″	−0·51	−0·09	−0·85
5·7″	−0·06	−0·99	+0·14

Type II (unconstrained)

W_{ij}'

11	22	33	12	13	23
0·32 (7)	0·32 (7)	0·18 (4)	0·19 (5)	0·16 (4)	0·9 (4)

Principal axes and directions

$\langle r_i\rangle$	Direction cosines*		
1·28μ	0·81	0·59	−0·05
1·56μ	0·52	−0·67	0·53
2·47μ	−0·28	0·45	0·85

Type I (constrained)

Z_{ij}'

11	22	33	12	13	23
4·1 (7)	4·1	4·1	1·4 (6)	1·4	1·4

Principal axes

$\langle\eta_i\rangle$	Directions of axes
3·16″	⊥ to threefold axis
3·16″	⊥ to threefold axis
3·19″	∥ to threefold axis

R index data (based on F^2)

	R_w	$n-m$
Isotropic	0·088	495
Type I	0·0750	490
Type II	0·0752	490
Type I, constrained	0·0760	494

* Direction cosines in this and the following Tables are given relative to an orthogonal axis system with directions parallel to **a***, **b** and **a*** × **b**.

Type II extinction is dominant. This belies the experimental facts in this case. On the other hand, the vector **D** which is relevant to Type I extinction is perpendicular to the scattering vector and rotates by 2π with α. Calculation of the intensity with the refined parameters from the full data set shows remarkably good agreement with the observations for the 202 and 101 reflections. The results for the 101 reflection are shown in Fig. 2. We conclude that the extinction in this case is better described as Type I than as Type II. The fine structure shown for the observed values in Fig. 2 cannot be reproduced by an ellipsoidal correction and suggests that the ellipsoidal model is but a first approximation to the truth.

One might expect that the extinction ellipsoid would have the point group symmetry of the crystal. This expectation does not generally appear to be exactly fulfilled, although the agreement is sometimes close. In this example, the expected rhombohedral symmetry is not obtained. To further test the significance of the deviation from trigonal symmetry, a refinement was carried out in which the tensor was constrained to have trigonal symmetry. The condition is that $Z_{11}=Z_{22}=Z_{33}$ and $Z_{12}=Z_{13}=Z_{23}$. The resulting values are $Z'_{11}=4{\cdot}1$ and $Z'_{12}=1{\cdot}4$. The weighted R value is 0·0760, a value which is significantly worse than that for the unconstrained refinement by the ratio test (Hamilton, 1965).*

The ellipsoids which describe the anisotropy of η are conveniently illustrated by the standard computer routines for illustrating thermal vibration ellipsoids. In Fig. 3 are illustrated the elliposids

$$(\mathbf{X}'\mathbf{Z}^{-1}\mathbf{X})=1$$

for the three refinements described above for $B_{12}P_2$.

Bis-(2-amino-2-methyl-3-butaneoximato)nickel(II)-chloride monohydrate

For monoclinic crystals of this compound, a set of 2120 neutron diffraction data was refined with both Type II anisotropic and isotropic extinction corrections (Schlemper, La Placa & Hamilton, 1969). The results are presented in Table 3. The extinction is seen to be not significantly anisotropic.

Table 3. *Extinction in a nickel complex (see text)*

Worst extinction: $F_{obs}^2/F_{calc}^2=0{\cdot}29$
$v=28{\cdot}16$ mm^3 $\lambda=0{\cdot}7107$ Å

Isotropic

$g'=1{\cdot}74$ (5)
$\eta=3{\cdot}35''$ or $r=1{\cdot}9\mu$

Type II Anisotropic

$\eta_1=\eta_2=\eta_3=1{\cdot}9\mu$

R index data (based on F^2)

	R	R_w
Isotropic and anisotropic	0·055	0·086

Hydrazinium sulfate

The extinction in the neutron diffraction study of this compound (Jønsson & Hamilton, 1968) was so severe that it was initially very difficult to locate the hydrogen atoms in an (observed – heavy atom) synthesis from the neutron data before an extinction correction was applied. An isotropic extinction correction allowed a structure solution and satisfactory refinement. Further improvement was however obtained when the extinction was allowed to be anisotropic. There was a very significant drop in the value of the weighted agreement index R_w. The Type II refinement gave a slightly better value for R_w. Refinements constraining the extinction parameters to orthorhombic symmetry gave significantly worse results with agreement indices halfway between the isotropic and unconstrained anisotropic results. The constrained and unconstrained ellipsoids for the Type II extinction refinements are more nearly alike than those for the Type I refinements. This fact and the fact that the R_w value is somewhat better lead us to conclude that the Type II model (particle size dominated) is most appropriate for this crystal. If so, the unusually large domain size of 22μ

* A further constrained refinement was carried out, based on only the data from the 101 reflection. This resulted in parameter values $Z_{11}=2{\cdot}5$ and $Z_{12}=-1{\cdot}5$. The determinant of **Z** was nonpositive, indicating that the data (from one reflection in this case) were not sufficiently good for the refinement of physically meaningful quantities.

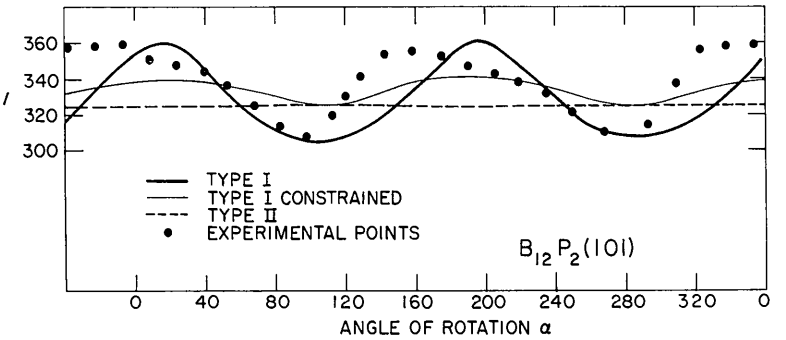

Fig. 2. Observed and calculated intensities for the 101 reflection in $B_{12}P_2$ as function of rotation around the diffraction vector. The parameters used in the calculations are based on least-squares refinement of a general set of reflections.

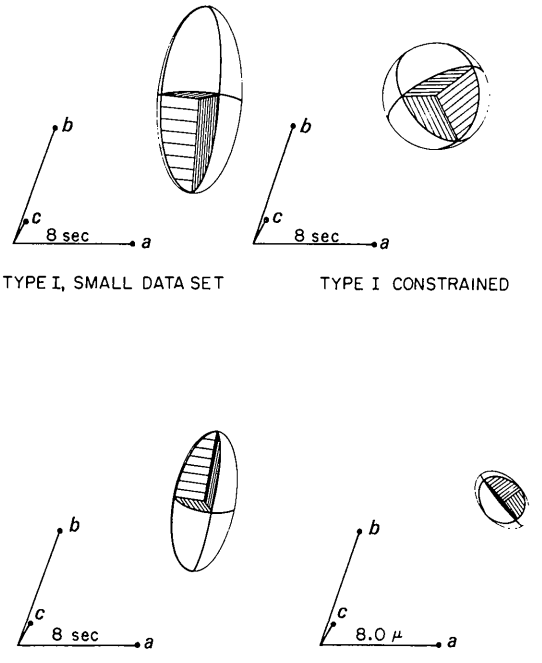

Fig. 3. Ellipsoids describing extinction for $B_{12}P_2$. The principal axes are r.m.s. mosaic spread parameters η in seconds for Type I and r.m.s. mean dimensions in microns for Type II. In the constrained refinement, rhombohedral symmetry was assumed for the tensor.

indicates that primary extinction is probably important, and confinement of the model to secondary extinction is not physically reasonable.

The pertinent quantities are given in Table 4, and the extinction ellipsoids for the four refinements are illustrated in Fig. 4.

A set of X-ray diffraction data on the same compound, but from a different crystallization batch, was also refined with a Type II extinction model. The results indicated a much smaller degree of crystal perfection (see Table 5 and Fig. 4).

*α-Deutero- and α-protooxalic acid dihydrate**

The X-ray data on the regular and the deuterated forms of oxalic acid dihydrate were collected by Delaplane & Ibers (1969). For both structures the results of the initial refinements were disappointing, as agreement factors remained at about 15% (Table 10). Introduction of an isotropic extinction parameter in the refinements led to a marked improvement. Nevertheless, the agreement factors were still larger than anticipated from a comparison of the intensities of symmetry-related reflections. Examination of the structure factor list revealed that reflections with $k=0$ for both compounds were generally undercorrected, while other reflections appeared to be overcorrected. An attempt

* Called α-DOX and α-POX, respectively.

Table 4. *Anisotropic extinction in hydrazinium sulfate (neutron data)*

Crystal data: orthorhombic, $a=8{\cdot}251$, $b=9{\cdot}159$, $c=5{\cdot}532$ Å
Worst extinction: $F_{obs}^2/F_{calc}^2=0{\cdot}12$; $v=3{\cdot}6$ mm^3; $\lambda=1{\cdot}073$ Å

Type I

Z_{ij}'

	11	22	33	12	13	23
Unconstrained	470 (59)	275 (52)	96 (26)	−56 (19)	−72 (16)	132 (26)
Constrained	463	305	118	0	0	0

Principal axes and directions

$\langle\eta_i\rangle$	Direction cosines			$\langle\eta_i\rangle$ constr.*
0·25″	0·89	−0·36	−0·27	0·27″
0·33″	0·44	0·82	0·37	0·33″
1·22″	0·09	−0·45	0·89	0·54″

Type II

W_{ij}'

Unconstrained	0·00563 (87)	0·00222 (30)	0·00233 (30)	−0·00091 (21)	0·00029 (15)	−0·00107 (18)
Constrained	0·00535	0·00173	0·00251			

Principal axes and directions

$\langle r_i\rangle$	Direction cosines			$\langle r_i\rangle$ constr.*
14μ	−0·95	+0·28	−0·16	15μ
19μ	−0·30	−0·60	+0·74	21μ
32μ	−0·11	−0·75	−0·65	26μ

R index data (based on F^2)

	R_w	$n-m$
No extinction	Unsatisfactory refinement	
Isotropic	0·1090	739
Type I	0·0974	734
Type II	0·0967	734
Type I (constr)	0·103	737
Type II (constr)	0·103	737

* Directions are along orthorhombic axes for constrained refinements.

to explain this anisotropy through the anisotropy of the crystal shape was made by using the numerical integration procedure developed by Hamilton (1963). This attempt led to a slight improvement, although a number of strong reflections remained poorly corrected. The strong reflections for both compounds were then recollected using very small crystals with volumes of 2×10^{-4} mm^3 and 13×10^{-4} mm^3 for α-DOX and α-POX respectively. Although extinction effects were effectively suppressed by this procedure the counting statistics were poor even for the stronger reflections, and little was gained from the additional experimental effort.

Introduction of the anisotropic extinction finally led to a more acceptable refinement of the initial set of data. Some results, summarized in Tables 6 and 8, illustrate the strong anisotropy of the correction. All elements of the **Z** tensors (Type I) are essentially zero except for Z_{22}, indicating that according to this interpretation the mosaic spread is very much smaller in planes with normals perpendicular to the *b* axis. The anisotropy of the extinction is slightly less pronounced for the neutron data on α-DOX, which were collected on an appreciably larger crystal (Coppens & Sabine, 1969). The results given in Table 7 show that the larger crystal was more nearly perfect. Thus particle size varied between 1·4 and 3·0μ, compared with 0·4 and 0·9μ for the X-ray data on the same compound. This situation is analogous to that found for hydrazinium sulfate (described above). This effect is not surprising,

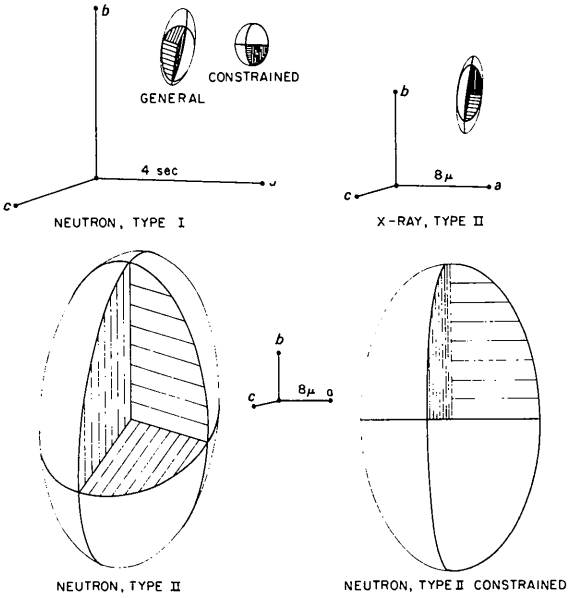

Fig. 4. Extinction ellipsoids for hydrazinium sulfate.

Table 5. *Anisotropic extinction in hydrazinium sulfate (X-ray data)*

Crystal data: orthorhombic, $a=8\cdot251$, $b=9\cdot159$, $c=5\cdot532$ Å
Worst extinction: $F_{obs}^2/F_{calc}^2=0\cdot21$, $v=0\cdot054$ mm^3, $\lambda=0\cdot7107$ Å

Type II extinction only

W_{ij}'

0·585 (98)	0·062 (11)	0·048 (7)	−0·045 (31)	−0·062 (19)	0·022 (7)

Principal axes and directions

$\langle r_i\rangle$	Direction cosines		
0·92μ	0·99	−0·09	−0·12
2·72μ	0·13	0·85	0·51
4·06μ	0·05	−0·52	0·85

R index data (based on F^2)

	R	R_w	*n*–*m*
No extinction	0·1700	0·1607	2516
Isotropic	0·0760	0·0907	2515
Type II	0·0574	0·0876	2510

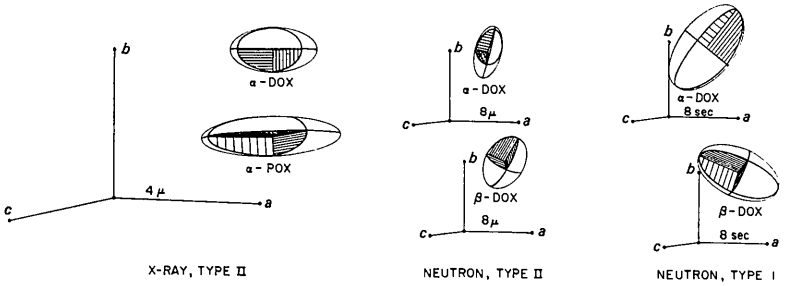

Fig. 5. Extinction ellipsoids for oxalic acid dihydrate.

because the larger crystals needed for neutron diffraction are usually grown more slowly and with more care than the small X-ray crystals. It follows that extinction will often be more severe for neutron data for this reason, not only because the path lengths inside the crystal are longer.

Extinction ellipsoids are shown in Fig. 5.

β-Deuterooxalic acid dihydrate

Neutron diffraction data on this compound were collected by Coppens & Sabine (1969). The results of the extinction refinement are given in Table 9. Extinction is again severe with particle sizes comparable with those obtained for α-DOX.

The extinction ellipsoids are reproduced in Fig. 5.

Table 6. *Anisotropic extinction in α-perdeuterooxalic acid dihydrate (X-ray data)*

Crystal data: monoclinic $a=6{\cdot}150$, $b=3{\cdot}612$, $c=12{\cdot}102$ Å, $\beta=106°38'$
Worst extinction: $F_{obs}^2/F_{calc}^2=0{\cdot}46$, $v=0{\cdot}0230$ mm³; $\lambda=0{\cdot}7107$ Å

Type I

Z_{ij}'

11	22	33	12	13	23
0·010 (10)	0·242 (16)	0·041 (18)	0·002 (7)	0·055 (14)	0·007 (11)

Tensor is non-positive definite and cannot be diagonalized.

Type II

W_{ij}'

4·1 (4)	16·0 (15)	4·3 (4)	−0·0 (7)	−1·9 (3)	−0·5 (7)

Principal axes and directions

$\langle r_i \rangle$	Direction cosines		
0·39μ	−0·00	1·00	−0·04
0·74μ	−0·76	0·03	0·65
0·90μ	+0·66	0·03	0·75

R index data (based on F^2)

	R_w	*n–m*
Isotropic	0·046	490
Type I	0·040	485
Type II	0·039	485

Table 7. *Anisotropic extinction in α perdeutero oxalic acid dihydrate (neutron data)*

Crystal data: monoclinic, $a=6{\cdot}150$, $b=3{\cdot}612$, $c=12{\cdot}102$ Å, $\beta=106°38'$
Worst extinction: $F_{obs}^2/F_{calc}^2=0{\cdot}21$; $v=3{\cdot}3$ mm³; $\lambda=1{\cdot}074$ Å

Type I

Z_{ij}'

11	22	33	12	13	23
3·1 (4)	2·3 (2)	5·3 (9)	−1·3 (4)	−1·1 (9)	0·8 (4)

Principal axes and directions

$\langle \eta_i \rangle$	Direction cosines		
2·6″	0·21	−0·25	−0·95
3·1″	−0·76	0·56	−0·32
5·1″	−0·61	−0·79	0·07

Type II

W_{ij}'

0·61 (6)	0·19 (3)	0·34 (4)	−0·10 (5)	−0·28 (6)	−0·0 (4)

Principal axes and directions

$\langle r_i \rangle$	Direction cosines		
1·38μ	0·95	−0·21	−0·25
2·18μ	0·08	−0·58	0·81
2·99μ	0·31	0·79	0·63

R index data (based on F^2)

	R_w	*n–m*
Isotropic	0·045	868
Type I	0·044	863
Type II	0·044	863

The effect of extinction on the positional and temperature parameters

The extinction effect introduces relatively small errors in the positional parameters. The bond lengths and angles for α-POX, for example, did not change by more than two standard deviations when the R value was reduced from 19·5 to 2·8% through the application of a number of different extinction procedures. At the same time the accuracy of the parameters increased considerably; standard deviations generally decreased by a factor 3 (Delaplane & Ibers, 1969). The situation is quite different, however, for the temperature factor parameters. The neutron data for both α-DOX and

Table 8. *Anisotropic extinction in α-oxalic acid dihydrate (X-ray data)*

Crystal data: $a=6{\cdot}119$, $b=3{\cdot}607$, $c=12{\cdot}057$ Å, $\beta=106°19'$
Worst extinction: $F_{obs}^2/F_{calc}^2=0{\cdot}38$; $v=0{\cdot}01856$ mm³; $\lambda=0{\cdot}7107$ Å

Type I

Z_{ij}'

11	22	33	12	13	23
−0·08 (1)	0·45 (3)	0·01 (3)	−0·01 (1)	0·07 (2)	0·01 (2)

Tensor is non-positive definite and cannot be diagonalized.

Type II

W_{ij}'

11	22	33	12	13	23
2·2 (2)	21·3 (2)	1·7 (2)	−1·5 (7)	0·1 (1)	−1·0 (8)

Principal axes and directions

$\langle r_i \rangle$	Direction cosines		
0·33μ	−0·08	+0·99	−0·08
0·98μ	0·73	+0·11	0·68
1·36μ	−0·68	0·00	0·73

R index data (based on F^2)

	R_w	$n-m$
Isotropic	0·058	482
Type I	0·044	477
Type II	0·039	477

Table 9. *Anisotropic extinction in β-deuterooxalic acid dihydrate (neutron data)*

Crystal data: monoclinic $a=10{\cdot}02$, $b=5{\cdot}05$, $c=5{\cdot}15$ Å, $\beta=99{\cdot}27°$
Worst extinction: $F_{obs}^2/F_{calc}^2=0{\cdot}20$; $v=4{\cdot}0$ mm³; $\lambda=1{\cdot}074$ Å

Type I

Z_{ij}'

11	22	33	12	13	23
2·4 (5)	4·8 (9)	4·2 (4)	1·1 (7)	−0·2 (4)	−1·4 (4)

Principal axes and directions

$\langle \eta_i \rangle$	Direction cosines		
2·4″	−0·22	−0·81	+0·55
3·0″	−0·45	−0·42	−0·79
4·6″	−0·87	+0·42	+0·28

Type II

W_{ij}'

0·24 (4)	0·19 (3)	0·35 (5)	−0·07 (3)	−0·05 (3)	−0·06 (2)

Principal axes and directions

$\langle r_i \rangle$	Direction cosines		
1·76μ	−0·14	+0·41	−0·90
2·06μ	−0·84	+0·43	+0·32
3·09μ	−0·52	−0·81	−0·29

R index data (based on F)

	R_w	$n-m$
Type I	0·038	637
Type II	0·039	637
Isotopic	0·039	642

Table 10. *R indices* (%)

	Before extinction		Isotropic		Anisotropic I		Anisotropic II	
	R	R_w	R	R_w	R	R_w	R	R_w
α-POX, X-rays								
F^2	19·5	14·8	6·5	5·8	3·6	4·4	2·8	3·9
F							2·1	2·0
α-DOX, X-rays								
F^2	17·2	12·9	4·1	4·6	2·5	4·0	2·8	3·9
F							2·3	2·0
α-DOX, neutrons								
F	6·2*	5·5*	4·4	4·5	4·3	4·4	4·3	4·4
β-DOX, neutrons								
F	5·8*	6·2*	4·0	3·9	3·8	3·8	3·8	3·9

* Excluding strong reflections.

β-DOX were at first subjected to a conventional refinement in which a large number of strong reflections (about 100 in each case) were excluded. The R values appeared acceptable (Table 10). After the extinction refinement had been developed, the results of the two treatments were compared, and a large increase in the diagonal elements of the thermal motion tensors was observed. As can be seen in Tables 11 and 12 the increase is positive for all the diagonal elements and typically about 7%, or roughly three standard deviations. Therefore, a proper allowance for extinction is especially important when the thermal parameters are to be used for the study of molecular motion.

It is of interest to note that the effect of extinction on least-squares parameters is very similar to the effect of uncorrected absorption (see for example Srivastava & Lingafelter, 1966).

Table 11. α-DOX. *Temperature parameters with* (E) *and without* (O) *extinction refinement*

		β_{11}	β_{22}	β_{33}
C	E	0·0163 (3)	0·0501 (9)	0·0036 (1)
	O	0·0146 (4)	0·0473 (14)	0·0032 (1)
	△	+0·0017	+0·0028	+0·0004
O(1)	E	0·0223 (4)	0·0915 (15)	0·0034 (1)
	O	0·0204 (6)	0·0871 (23)	0·0031 (1)
	△	+0·0019	+0·0044	+0·0003
O(2)	E	0·0217 (4)	0·0894 (15)	0·0043 (1)
	O	0·0199 (5)	0·0853 (24)	0·0038 (1)
	△	+0·0018	+0·0041	+0·0005
O(3)	E	0·0222 (4)	0·0889 (15)	0·0042 (1)
	O	0·0210 (6)	0·0839 (23)	0·0038 (1)
	△	+0·0012	+0·0050	+0·0004
D(1)	E	0·0260 (4)	0·0895 (16)	0·0047 (1)
	O	0·0252 (7)	0·0839 (24)	0·0045 (2)
	△	+0·0008	+0·0056	+0·0002
D(2)	E	0·0287 (5)	0·1026 (17)	0·0055 (1)
	O	0·0272 (7)	0·0964 (25)	0·0051 (2)
	△	+0·0015	+0·0062	+0·0004
D(3)	E	0·0294 (5)	0·1103 (19)	0·0089 (1)
	O	0·0278 (8)	0·1046 (30)	0·0086 (2)
	△	+0·0016	+0·0057	+0·0003
Average variation		6·7%	5·4%	8·2%

Table 12. β-DOX. *Temperature parameters with* (E) *and without* (O) *extinction refinement*

		β_{11}	β_{22}	β_{33}
C	E	0·0058 (1)	0·0241 (4)	0·0291 (4)
	O	0·0051 (1)	0·0213 (5)	0·0269 (5)
	△	+0·0007	+0·0028	+0·0022
O(1)	E	0·0077 (1)	0·0339 (5)	0·0467 (6)
	O	0·0072 (2)	0·0308 (7)	0·0449 (8)
	△	+0·0005	+0·0031	+0·0018
O(2)	E	0·0079 (1)	0·0339 (6)	0·0375 (5)
	O	0·0073 (2)	0·0311 (8)	0·0352 (7)
	△	+0·0006	+0·0028	+0·0023
O(3)	E	0·0100 (2)	0·0503 (7)	0·0487 (7)
	O	0·0095 (2)	0·0468 (10)	0·0461 (9)
	△	+0·0005	+0·0035	+0·0026
D(1)	E	0·0084 (1)	0·0382 (6)	0·0461 (6)
	O	0·0081 (2)	0·0354 (8)	0·0433 (8)
	△	+0·0003	+0·0028	+0·0028
D(2)	E	0·0120 (2)	0·0476 (7)	0·0398 (6)
	O	0·0113 (2)	0·0442 (9)	0·0368 (8)
	△	+0·0007	+0·0034	+0·0030
D(3)	E	0·0096 (1)	0·0411 (6)	0·0480 (6)
	O	0·0088 (2)	0·0375 (9)	0·0448 (9)
	△	+0·0008	+0·0036	+0·0032
Average variation		7·0%	8·5%	6·2%

Concluding remarks

In most of the compounds described here the R values are very similar for the Type I and Type II treatments. Fortunately, the positional and temperature parameters are equal to within one standard deviation for the two treatments. It is therefore of no consequence for the structural analyses whether Type I or Type II is closer to reality. In many cases extinction will be affected both by mosaic spread and particle size and neither extreme will be entirely correct. Only in the X-ray study of α-POX can a clear choice be made on the basis of the R value alone (Table 8), while the φ dependence of the intensity of the 202 and 101 reflections of $B_{12}P_2$ can only be explained on the basis of mosaic spread dominated extinction. It would be of considerable interest to compare such conclusions with wavelength dependence measured on the same crystals.

Such measurements can also lead to a determination of the nature of the extinction (Zachariasen, 1968*b*).

The parameters obtained with the present method are physically reasonable, although detailed comparison with other methods of determining crystal texture, to be performed on the same specimen, is desirable.

We conclude that the significance of the extinction parameters in improving the agreement between observed and calculated structure factors is convincing. They should be included in least-squares refinement of extinction-affected data whenever accurate positional parameters and reliable temperature parameters are desired.

We would like to thank several of our co-workers for supplying data discussed in the examples above. In particular, Sam J. LaPlaca carried out the entire extinction analysis for $B_{12}P_2$.

APPENDIX

Symbol table

$A(\mu)$ or A The absorption correction $\frac{1}{v}\int \exp(-\mu(T_1+T_2))d\tau$. e^2/mc^2 The X-ray scattering amplitude for a single electron in cm.

D A unit vector with components D_i, perpendicular to the plane of diffraction.

F The structure factor in cm cell^{-1} for neutrons; in electrons cell^{-1} for X-rays.

F_c The absolute calculated structure factor, not including a scale factor.

F_k The scaled structure factor: $F_k = kF_c$.

g Isotropic extinction parameter or equivalent isotropic extinction parameter as defined in Table 1.

G Matrix of a space in which the vectors **D** and **N** are defined.

I_0 The intensity of the direct beam inside the crystal in cm^{-2}sec^{-1}.

I The intensity of the scattered beam inside the crystal in cm^{-2}sec^{-1}.

$\mathscr{I}_0$ The intensity of the incident beam before it strikes the crystal, cm^{-2}sec^{-1}.

k The scale factor.

K The polarization factor for the parallel component of polarization in the incident beam. 1 for neutrons, $\cos^2 2\theta$ for X-rays.

N Unit vector with components N_i, in the diffraction plane and perpendicular to the incident beam.

p_1 $1+K$, for unpolarized incident radiation.

p_2 $1+K^2$, for unpolarized incident radiation.

P Any parameter other than extinction or scale.

$\mathscr{P}$ Integrated intensity of a Bragg reflection in sec^{-1}.

$P(\varepsilon)$ Power of the diffracted beam in a particular direction ε.

$\mathscr{P}_k$ Integrated intensity in the kinematic approximation of a Bragg reflection, sec^{-1}.

Q Average scattering cross-section per unit volume of crystal, cm^{-1}.

Q_0 Same as Q for $K=1$.

r The radius of a spherical domain.

$r(\mathbf{N})$ The semi-length of a line through the center of an ellipsoid in a direction defined by **N**.

t_1 Distance in the incident beam direction in a single domain, cm.

T_1 Distance in the incident beam direction in the entire crystal, cm.

t_2 Distance in the diffracted beam direction in a single domain, cm.

T_2 Distance in the diffracted beam direction in the entire crystal, cm.

$\bar{t}$ Mean length of beam path in a single domain.

$\bar{T}_0$ Mean length of beam path in the entire crystal.

$\bar{T}$ Absorption-weighted mean length of beam path in the entire crystal.

v Volume of the crystal, cm^3 .

V Volume of the unit cell, 10^{-24}cm^3.

W A tensor with components W_{ij} which describes the anisotropy of domain size.

$\bar{x}_0$ A dimensionless quantity giving average strength of scattering; defined in equation (12).

X A vector with components X_i.

y The extinction correction $y = \mathscr{P}/\mathscr{P}_k$.

Z A tensor with components Z_{ij} which describes the anisotropy of mosaic spread.

β A dimensionless quantity defined in equation (13).

γ $= -2(p_2/p_1)(\bar{T}/\sin 2\theta)(\lambda^3/V^2)$ cm^{-2} if F is in 10^{-12} cm cell^{-1}; if F is in electrons, divide by $12{\cdot}593 = (e^2/mc^2)^{-2}$.

Δ Angular deviation of the mosaic block position from the mean in an isotropic distribution, or magnitude of the deviation in a particular direction for an anisotropic distribution.

δ The least-squares estimated correction in a parameter.

δ_{ij} $=1$ for $i=j$; 0 for $i \neq j$.

ε Direction of a diffracted beam.

η Mosaic spread parameter (standard deviation of a Gaussian distribution) radians.

$\eta(\mathbf{D})$ Mosaic spread parameter around a direction **D** when the Gaussian distribution is anisotropic.

θ The Bragg angle.

λ Wavelength of the radiation, 10^{-8} cm.

Λ Eigenvalues of **W** or **Z**.

μ The linear absorption coefficient in cm^{-1}.

π The usual meaning.

$\sigma(\varepsilon)$ Cross section per unit volume and intensity, cm^{-1}; analogous to Q but in a particular direction ε.

$d\tau$ Differential for integration over all crystal volume elements.

$\varphi(\sigma)$ Extinction correction for a single domain in a particular direction.

$\psi(\Delta)$ Mosaic spread distribution function.

References

COPPENS, P. & SABINE, T. M. (1969). *Acta Cryst.* B **25**, 2442.
DELAPLANE, R. G. & IBERS, J. A. (1969). *Acta Cryst.* B **25**, 2423.
HAMILTON, W. C. (1957). *Acta Cryst.* **10**, 629.
HAMILTON, W. C. (1963). *Acta Cryst.* **16**, 609.
HAMILTON, W. C. (1965). *Acta Cryst.* **18**, 502.
IBERS, J. A. (1968). Private communication.
JØNSSON, P.-G. & HAMILTON, W. C. (1968). Unpublished results.
LA PLACA, S. J. (1968). Private communication.
LARSEN, A. C. (1967). *Acta Cryst.* **23**, 664.
SCHLEMPER, E. O., LA PLACA, S. J. & HAMILTON, W. C. (1968). Unpublished results.
SRIVASTAVA, R. C. & LINGAFELTER, E. C. (1966). *Acta Cryst.* **20**, 918.
ZACHARIASEN, W. H. (1963). *Acta Cryst.* **16**, 1139.
ZACHARIASEN, W. H. (1967). *Acta Cryst.* **23**, 558.
ZACHARIASEN, W. H. (1968*a*). *Acta Cryst.* A **24**, 212.
ZACHARIASEN, W. H. (1968*b*). *Acta Cryst.* A **24**, 421.
ZACHARIASEN, W. H. (1969). *Acta Cryst.* A **25**, 102.

Acta Cryst. (1970). A **26**, 83

A Re-evaluation of Bonding Features in Diamond and Silicon

BY J. F. MCCONNELL AND P. L. SANGER*

Crystallographic Laboratory, School of Physics, University of New South Wales, Sydney, Australia

(*Received* 14 *April* 1969 *and in revised form* 30 *July* 1969)

Published X-ray powder measurements on diamond and three different sets of published X-ray data on silicon have been re-analysed for bonding features using full-matrix least-squares refinement combined with a statistical analysis of the results obtained. In all cases a highly significant improvement in the fit between observed and calculated structure factors was obtained by introducing a tetrahedral distortion of the spherical 'prepared' charge distribution, but subsequent introduction of a fourth-order cubic distortion proved to be highly significant only for the diamond data and one set of the silicon data. Hartree–Fock calculations gave a better fit to the diamond measurements than calculations based on Hartree–Fock–Slater wave functions. The necessity for placing restrictions on the form of the radial functions associated with the non-spherical distortions, the large estimated standard deviations of the distortion parameters and the dependence of the parameter values on the set of basis wave functions chosen to describe the spherical 'prepared' charge distribution indicate the need for exercising caution in analysing the experimental measurements for bonding features.

Introduction

The diamond powder measurements of Göttlicher & Wölfel (1959) have recently been analysed for bonding features by Dawson (1967*b*) using a general structure factor formalism, Dawson (1967*a*). Similar bonding features in silicon have also been described by Dawson (1967*c*), who analysed the three different sets of X-ray data for silicon at present available† in the literature, *i.e.* the powder measurements of Göttlicher & Wölfel (1959) and the perfect single-crystal measurements of DeMarco & Weiss (1965) and Hattori, Kuriyama, Katagawa & Kato (1965).

Another approach, reported by Weiss (1964) and DeMarco & Weiss (1965), has also been used to analyse the X-ray data on diamond and silicon for bonding features. The similarities and differences between this and the approach of Dawson (1967*a*) are discussed in detail by Dawson & Sanger (1967) where it is shown that only the latter's approach permits adequate interpretation of the experimental data.

In the present paper the experimental measurements for diamond and silicon have been re-analysed for the features of bonding using the formalism of Dawson (1967*a*). However, this time the method of least squares has been used to determine the various parameters associated with the non-spherical distortions of the spherical 'prepared' charge distribution and the significance tests of Hamilton (1964, 1965*a*) are applied before discussing the bonding features in these compounds.

Theory

The space group of diamond is $Fd3m$ (O_h^7) and the complete lattice may be built up from two atomic positions with point group symmetry $\bar{4}3m$ (T_d) combined with the normal face-centred translations.

Application of the formalism of Dawson (1967*a*) shows that, in the calculation of structure factors for the diamond lattice, allowance must be made for non-

* Present address: Applied Mathematics and Computing Section, Australian Atomic Energy Commission Research Establishment, Private Mailbag, Sutherland, N.S.W.2232, Australia.

† Hart & Milne (1969) have recently reported the measurement of the 220 reflexion in silicon. However, their results have not been used here since they do not represent a complete set of data for silicon.